Liquid Crystals
Publication details, including instructions for authors and subscription information:
http://www.informaworld.com/smpp/title~content=t713926090

Polarization holographic techniques: a method to produce diffractive devices in polymer dispersed liquid crystals

A. Mazzulla[a]; A. Dastoli[a]; G. Russo[a]; L. Lucchetti[b]; G. Cipparrone[a]
[a] Istituto Nazionale per la Fisica della Materia, c/o Dipartimento di Fisica Università della Calabria, 87036 Rende (CS), Italy, [b] Istituto Nazionale per la Fisica della Materia, c/o Dipartimento di Fisica e Ingegneria dei Materiali e del Territorio - Università di Ancona, Via Brecce Bianche, 60131 Ancona, Italy,

Online publication date: 11 November 2010

To cite this Article Mazzulla, A. , Dastoli, A. , Russo, G. , Lucchetti, L. and Cipparrone, G.(2003) 'Polarization holographic techniques: a method to produce diffractive devices in polymer dispersed liquid crystals', Liquid Crystals, 30: 1, 87 — 92
To link to this Article: DOI: 10.1080/0267829021000051737
URL: http://dx.doi.org/10.1080/0267829021000051737

LIQUID CRYSTALS, 2003, VOL. 30, NO. 1, 87–92

Polarization holographic techniques: a method to produce diffractive devices in polymer dispersed liquid crystals

A. MAZZULLA, A. DASTOLI, G. RUSSO, L. LUCCHETTI† and G. CIPPARRONE*

Istituto Nazionale per la Fisica della Materia,
c/o Dipartimento di Fisica Università della Calabria, 87036 Rende (CS), Italy
†Istituto Nazionale per la Fisica della Materia,
c/o Dipartimento di Fisica e Ingegneria dei Materiali e del Territorio –
Università di Ancona, Via Brecce Bianche, 60131 Ancona, Italy

(*Received 24 June 2002; in final form 5 August 2002; accepted 25 September 2002*)

We report a study of holographic gratings recorded by exposing a homogeneous mixture of prepolymer and liquid crystal to polarization light patterns. The method is based on the alignment control of the liquid crystal domains during the photo-induced polymerization process. In contrast, the usual methods to write diffraction gratings in polymer dispersed liquid crystals are based on an intensity holographic technique that controls the polymerization process. The polarization patterns here are made using different geometries: in particular we report results from exposure to polarization patterns realized by the superposition of two waves having orthogonal linear polarizations, or two waves having opposite circular polarizations. Analyses of the recorded gratings are reported.

1. Introduction

The development of holographic and diffractive optics technology in the last few years has involved liquid crystals and polymer composite materials. Electrically and optically switchable holographic gratings in polymer dispersed liquid crystals (PDLCs) have been extensively studied [1–7].

In particular, more attention relating to holographic applications has been paid to PDLC systems produced by means of polymerization induced phase separation (PIPS) in which the polymerization process is induced by light exposure. The interest in these materials lies in the possibility of combining the ease of holographic recording in photopolymeric systems with index modulation control through orientation of the liquid crystal induced by an applied voltage.

Recently [8, 9] we have reported the observation of holographic grating formation in PDLCs on exposing a homogeneous mixture of prepolymer and liquid crystal to a polarization light pattern made by spatial superposition of two laser beams having orthogonal linear polarizations at 45° with respect to the incidence plane. The method is based on alignment control of the liquid crystal domains during the polymerization process instead of on polymerization control, as in the usual method. The idea behind this technique comes from the possibility of obtaining alignment control of the liquid crystal inside the domains through photoalignment (of the polymer or the liquid crystal) during the photoinduced polymerization phase separation. Such a process, in the case of polarization holography, takes place uniformly due to the spatially constant light intensity distribution. This peculiarity is considered to improve the stability of the recorded structures in the film and the efficiency of electrical switching of the grating.

In this paper we show the possibility of recording holographic gratings in polymer liquid crystal composite materials by using two polarization patterns obtained by superimposing two waves with orthogonal linear polarizations or two waves with opposite circular polarizations. The first interference pattern is composed of a sequence of regions in which the polarization varies continuously from linear to circular along the grating wave vector direction figure 1 (*a*). The second pattern is made by a rotating linear polarization, figure 1 (*b*). In both configurations we were able to obtain diffraction gratings. A detailed experimental study of the recorded structures is given, in particular concerning the polarization properties, the dynamics of the efficiency, the electrical swtiching and the morphology.

*Author for correspondence; e-mail: cipparrone@fis.unical.it

Liquid Crystals ISSN 0267-8292 print/ISSN 1366-5855 online © 2003 Taylor & Francis Ltd
http://www.tandf.co.uk/journals
DOI: 10.1080/0267829021000051737

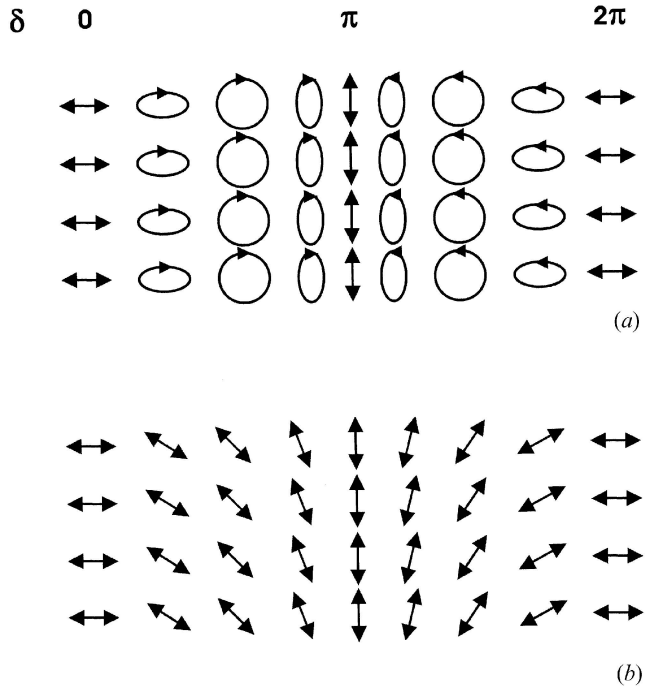

Figure 1. Polarization modulations of the interference light field recording the gratings in our geometries. (*a*) Two orthogonal linearly polarized beams, 45° and −45°, (*b*) two opposite circularly polarized beams.

2. Experimental

In our experiment the gratings are written by exposing the liquid crystal–prepolymer syrup to a light pattern obtained by superposition of two waves having orthogonal linear polarizations (in particular it is noted that the beams are polarized at angles of +45° and −45° with respect to the plane of incidence) or two opposite circular polarizations.

When two orthogonal, linearly polarized beams cross at a small angle θ, the modulation pattern produced can be evaluated as follows. If $\mathbf{E}_{+45}$ is the field of the linearly polarized wave at +45° and $\mathbf{E}_{-45}$ is the field at −45°, the resultant field, $\mathbf{E} = \mathbf{E}_{+45} + \mathbf{E}_{-45}$, keeps a polarization distribution as sketched in figure 1 (*a*) and can be written as a Jones vector

$$\mathbf{E} = \frac{2}{\sqrt{2}} \begin{vmatrix} \cos(\theta/2)\cos(\delta/2) \\ \mathrm{i}\sin(\delta/2) \end{vmatrix} \qquad (1)$$

where $\delta = 2\sin(\theta/2)(2/\lambda)x$ is the phase difference at position x of the writing waves, and λ is the laser wavelength.

For two opposite circular polarizations the resulting field $\mathbf{E} = \mathbf{E}_{\mathrm{cl}} + \mathbf{E}_{\mathrm{cr}}$ (where $\mathbf{E}_{\mathrm{cl}}$ is the field of the left circularly polarized wave and $\mathbf{E}_{\mathrm{cr}}$ is the field of the right circularly polarized wave) is linearly polarized and its distribution, see figure 1 (*b*), can be written as

$$\mathbf{E} = \frac{2}{\sqrt{2}} \begin{vmatrix} \cos(\delta/2) \\ -\sin(\delta/2) \end{vmatrix}. \qquad (2)$$

The material consists of a prepolymer syrup of a homogeneous mixture of monomer (PWL01 B-component, PN393, 52.9 wt %), nematic liquid crystal (PWL01 C-component of a TL-mixture series, 47 wt %), both from E. Merck, and a small amount of photoinitiator dye, Bengal Rose 0.1 wt %. The cells assembled using ITO coated glass plates were 10 μm thick.

The experimental set-up for holographic recording is depicted in figure 2. Two Ar-ion laser beams ($\lambda = 514.5$ nm) having equal intensities cross at an angle $\theta = 3.2°$, corresponding to a spatial periodicity of 7 μm. The film is placed in the superposition region of the beams. In this configuration the intensity distribution on the sample is quite uniform, while the polarization state changes as shown in figures 1 (*a*) and 1 (*b*) for two linear or two circular polarizations, respectively. Holographic gratings are recorded for light intensity values ranging from 50 to 300 mW cm^{-2} and an exposure time of a few minutes. A linearly polarized He-Ne laser beam ($\lambda = 632.8$ nm) is used as a probe beam in order to investigate the light fields diffracted by the grating. The diffraction efficiency η, defined as the ratio of the i-th diffracted beam intensity to the total transmitted intensity, $\eta_{\pm i} = I_{\pm i}/I_{\mathrm{T}}$, is measured for both p (in the incidence plane) and s (orthogonal to p) polarized probe beams. When a final steady value is reached, the efficiency of each polarization is measured; the η_{p} value is always found to be higher than η_{s}, except at low intensity where they are almost the same. Figures 3 (*a*) and 3 (*b*) represent the efficiency function of the writing intensity for the two configurations, linear and circular, respectively. In these graphs the data points are the efficiencies for the p and s polarized probe beams after the writing process. In the first graph, related to the linear configuration, the p efficiency monotonically

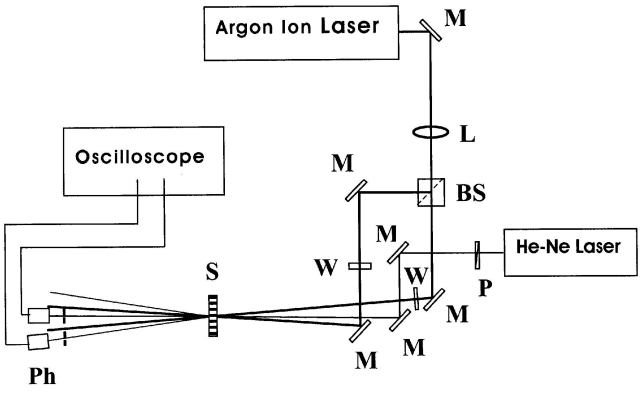

Figure 2. Experimental set-up: M mirror, L lens, BS beam splitter, W waveplate, P polarizer, S sample, Ph photodiodes.

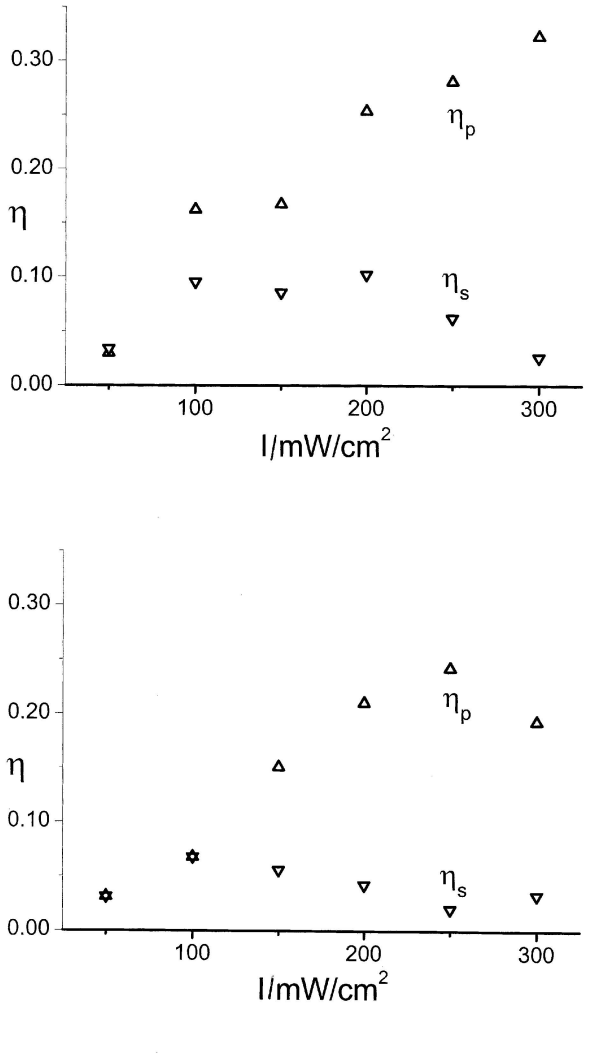

Figure 3. Maximum efficiency values for s and p probe polarization states at several incident intensities. (*a*) The writing polarization pattern is sketched in fig. 1a; (*b*) the writing polarization pattern is sketched in fig. 1b.

increases with intensity while the s efficiency has a maximum at about 150 mW cm^{-2}. In the second configuration, the p efficiency reaches its maximum around 250 mW cm^{-2} where, on the contrary, the s efficiency has its minimum.

It is worth noting that η_s is comparable to η_p only at intensities below about 100 mW cm^{-2}; then at higher intensities the two efficiency values split apart. Analyses of the diffracted probe beams confirm that they have the same polarization state as the incident beam for both configurations.

Figures 4 and 5 show polarizing optical microscopy (POM) images between crossed polarizers of two gratings recorded at 200 mW cm^{-2} intensity. Figures 4(*a*) and 5(*a*) are taken when the grating wave vector makes an angle of 0° with respect to the incident light vector, while in figures 4(*b*) and 5(*b*) the angle is 45° and in figures 4(*c*) and 5(*c*) it is 90°. The images indicate that the liquid crystal inside the cavities, corresponding to the bright stripes of figures 4(*b*) and 5(*b*), is well aligned along the direction parallel to the wave vector of the grating, as checked by optical compensation techniques [8]. Moreover, the spacing of the stripes matches the spatial periodicity of the interference pattern. The main difference between the two sequences of images is the better constrast of the grating written with the orthogonal linear polarizations.

In figure 6 we report the dynamics of the first order diffraction efficiency during the writing process, for linear (*a*) and circular (*b*) configurations. The Ar-ion laser is turned on at time $t = 0$ s, the probe diffracted beams arise after roughly two min, and at the same time scattered light appears owing to the occurrence of phase separation. The p diffraction efficiency increases monotonically reaching its maximum after a few min; afterwards, a slow decrease over tens of min towards a stable value is observed (outside the graph scale). On the contrary, the s polarized efficiency gives a maximum after about three min and a subsequent decrease.

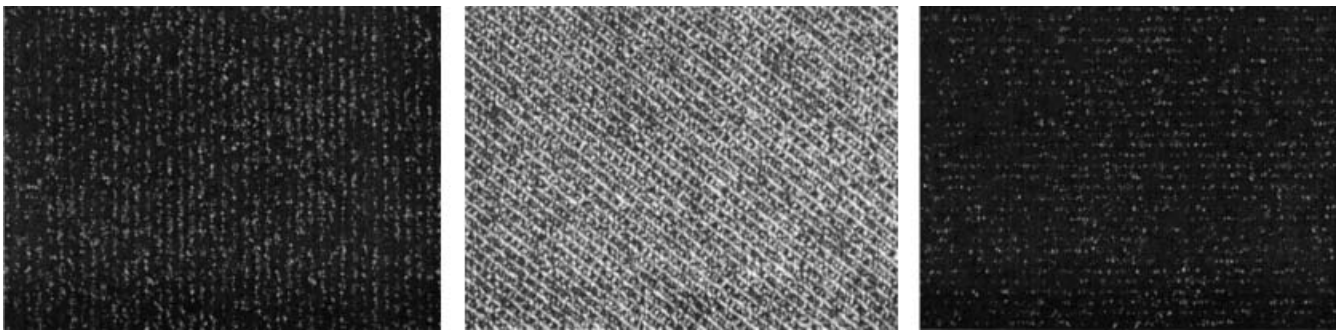

(*a*) (*b*) (*c*)

Figure 4. POM images, between crossed polarizers, when the grating wave vector make angles, with respect to the incident light vector, of 0° (*a*), 45° (*b*) and 90° (*c*). The writing pattern is given by orthogonal linear polarizations, figure 1(*a*).

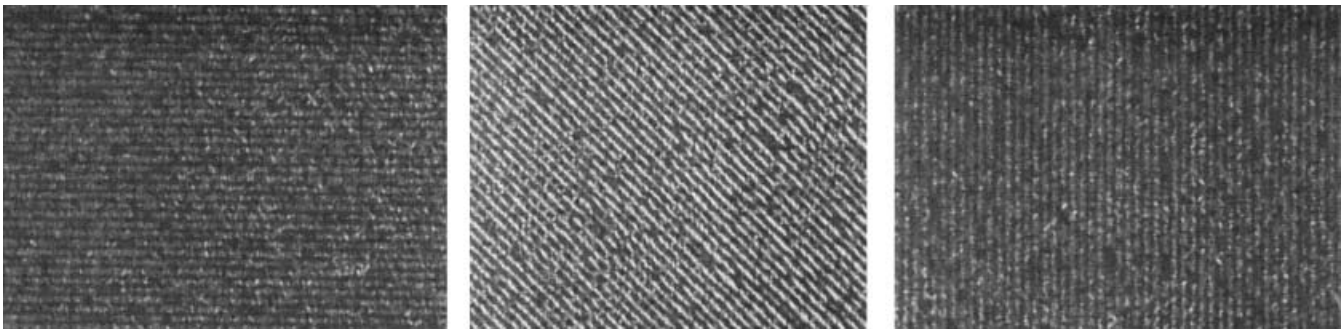

(*a*) (*b*) (*c*)

Figure 5. POM images, between crossed polarizers, when the grating wave vector make angles, with respect to the incident light vector, of 0° (*a*), 45° (*b*) and 90° (*c*). The writing pattern is given by orthogonal circular polarizations, figure 1 (*b*).

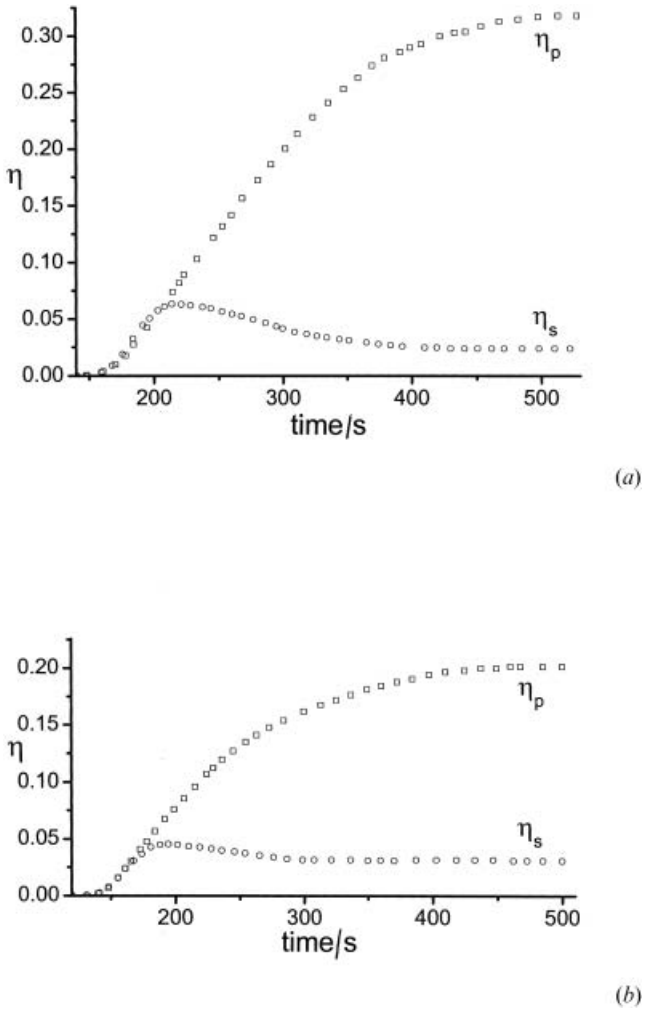

Figure 6. Temporal evolution of the first order diffraction efficiency for p and s polarizations of the probe beam; the writing intensity is 300 mW cm^{-2}. The polarization patterns are: ±45° linear (*a*), and opposite circular (*b*).

In our experimental conditions, the uniform illumination during the phase separation and the grating recording prevents anisotropic molecular diffusion processes affecting the periodic structure of the grating. Moreover, additional amplitude or phase grating formation, originating from density or concentration modulation, can be excluded, even if in the ±45° linear pattern an unpredicted surface relief grating has been observed. For this reason more efficient electrical switching of the grating is expected. In fact, as the liquid crystal orientation inside the domains is the only factor responsible for the grating structure, a suitable applied voltage can produce very efficient optical switching.

Figure 7 shows the POM images in the same geometry as that of figure 4 (*b*), without an applied voltage in figure 7 (*a*), and on applying an a.c. voltage of 65 V at 1 kHz in figure 7 (*b*). At this voltage a complete temporary optical erasure of the grating is obtained.

From the analysis of the efficiency, we observe that the diffracted probe beams nearly disappear. The modulation of the efficiency is clearly shown in figure 8, where a driving voltage of 65 V at 100 Hz is applied to the sample. Gratings written with the circular polarization pattern also present such features; the difference lies in a less deep modulation of the efficiency.

In order to investigate liquid crystal segregation after the polymerization process, scanning electron microscopy was applied using sections of irradiated PDLC samples. The morphology of the gratings was also investigated by scanning electron microscopy (SEM). After removing one of the two glass substrates, samples were placed under vacuum for one night to allow the liquid crystal near the surface to evaporate. In this way scanning electron micrographs allowed us to visualize the holes left by the liquid crystal. Subsequently, samples were coated with a thin film of conductive metal (10 nm of gold), by using a sputter coater. Sample cross-sections were obtained by fracturing the cells in liquid nitrogen.

All the analysed gratings show the presence of a channel structure through the whole depth. A channel morphology is indeed quite common in laser cured

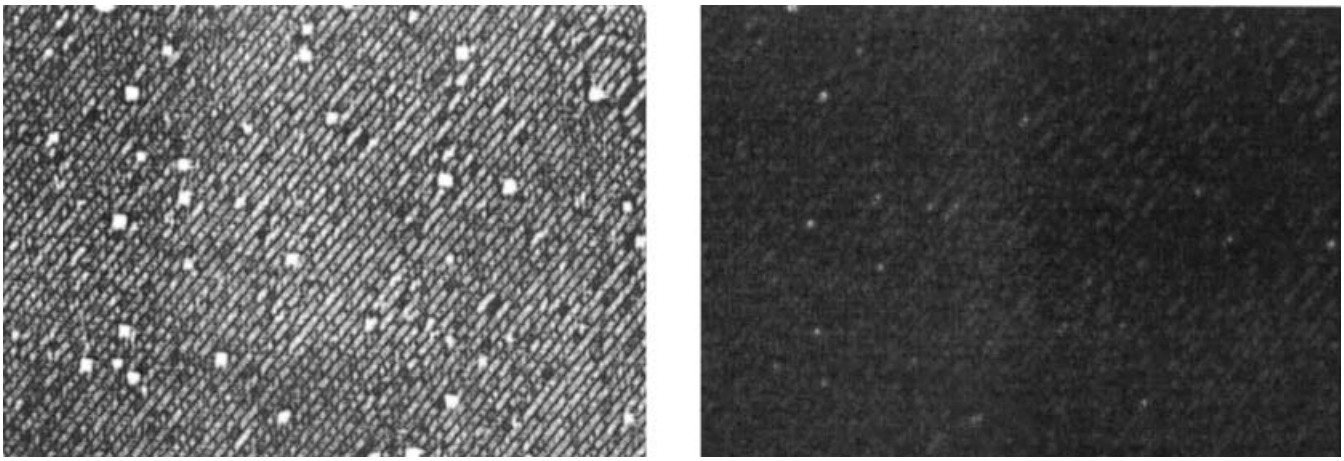

(*a*) (*b*)

Figure 7. POM images, between crossed polarizers, with the grating wave vector making a 45° angle with respect to the incident light vector: without applied voltage (*a*) and applying 65 V at 1 kHz frequency (*b*).

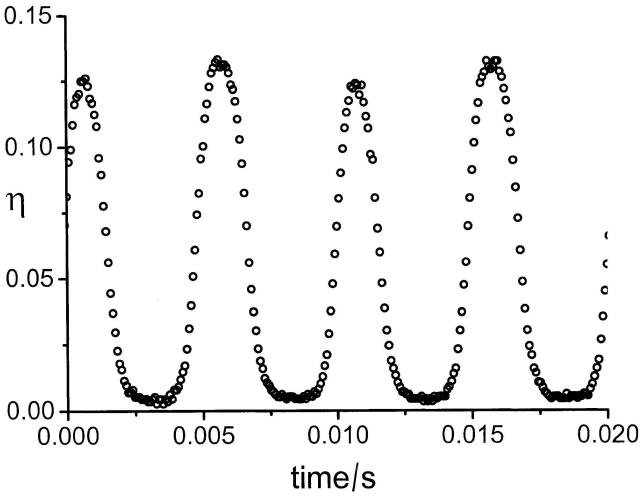

Figure 8. Efficiency modulation of the first order diffracted beam on applying 65 V at 100 Hz.

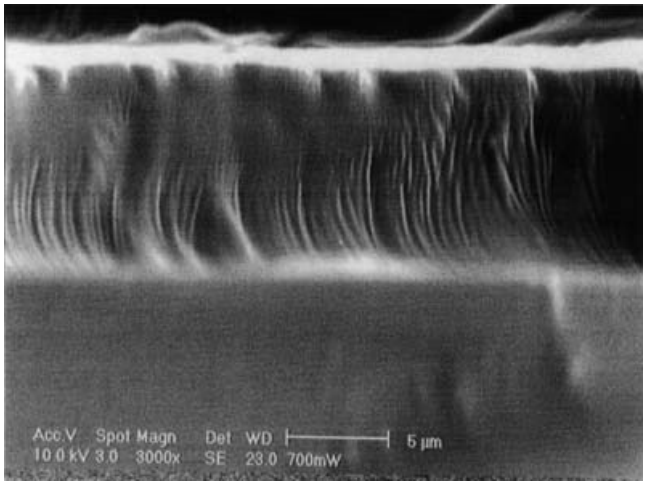

Figure 9. SEM micrograph of a section of grating written at 300 mW cm^{-2} intensity.

PCLCs [10, 11]. In particular, the formation of polymeric channels has been detected in the case of laser curing with incident powers of the order of some hundreds of mW. Channel formation has been ascribed to the freezing of thermal convective motion caused by the strong thermal gradients that arise in the case of coherent curing. Both X-ray diffraction and conoscopy have provided evidence that the liquid crystal molecules can spontaneously align along the channels during the phase separation process, thus giving rise to transparent samples. Figure 9 shows a section of a grating written at 300 mW cm^{-2} intensity. The region corresponding to the grating shows a quite regular morphology; no droplets are present and only a channel structure is visible. The average dimension of the channels is of the order of 0.1 μm. These preliminary results, although difficult to explain, allow us to exclude any periodical structure of droplets in the morphology that could correspond to the optical gratings.

3. Discussion and conclusions

The main results of our investigations can be summarized as follows. Permanent gratings in PDLC films are recorded by polarization light patterns. At intensities lower than 50 mW cm^{-2} no gratings are produced, even for long exposure times, although the polymerization process takes place. This observation, common to both configurations, could be related to the liquid crystal domain size (obtained for this intensity value) with respect to the dimension of the regions in which the polarization can be assumed to be uniform.

All the gratings have a strong anisotropy of the diffraction efficiency. In both configurations, at low intensity ($\sim 50\,\mathrm{mW\,cm^{-2}}$), p and s efficiencies have similar values $\eta_s \cong \eta_p$, while at higher intensity $\eta_p > \eta_s$. Generally, the anisotropy tends to grow with the intensity. The main differences between the two configurations consist of a higher p efficiency and a larger anisotropy $(\eta_p - \eta_s)$ in the linear polarization pattern with respect to the circular pattern, as can be seen in figures 3(*a*) and 3(*b*).

The polarization state of all beams transmitted from the gratings is identical to that of the incident beam. Time evolutions of the grating efficiency during the writing process are about the same for both configurations. The above mentioned features, related to the optical characteristics for both writing configurations, are not those expected if the effect involved were just a photoalignment of the materials. In fact, substantial differences should be evident between the gratings recorded by the two polarization patterns [12]. These observations therefore indicate that the anisotropy of the pattern (stripes having the same polarization, see figure 1) could influence in some way the configuration of the liquid crystal domains. This arrangement is thought to be controlled by polymer chain growth along a preferred direction during the writing process.

The recorded holographic structures have long term stability, more than six months up to now. Almost total electrical modulation of the diffraction properties is obtained on applying an alternating voltage to the transparent electrodes on the cell plates. The rise and fall times of the modulation (figure 8) for the linear configuration are ~ 2 ms, which is actually equal to the usual response time of the PDLC structure. The SEM analyses confirm the absence of a grating-like distribution of droplet size or shape corresponding to the optical gratings.

It seems evident from the experimental results that refractive index modulation is predominantly due to the liquid crystal orientation inside the domains. In particular, the permanence of the diffracting structure after the writing process, and the possibility of totally modulating the efficiency by an applied voltage, suggest that the optical orientation occurring during the illumination (and the phase separation) induces a particular arrangement of the liquid crystal–polymer interface. This configuration, fixed by the polymerization, persists even after removing the writing polarization pattern. It is not yet clear if the optical field during the polymerization phase separation process orients the liquid crystal and/or the monomer molecules. The observation of polymer alignment along a preferred direction during the cross-linking process, if photoreaction is induced by exposure to polarized light, cannot exclude any involvement of the polymer in the reorientation of the liquid crystal domains [13, 14]. Nevertheless, since the domain interface is a more or less extended region over which the concentration of the components changes in a continuous way, such a variation can be attributed to a combination of the two photoinduced effects described before.

In conclusion we describe the possibility of producing diffraction gratings in PDLCs using holographic polarization techniques. It seems that the hypothesis based only on the photoinduced linear birefringence does not fully support the experimental evidence; more complex mechanisms must take place during the gratings writing process.

The complexity of the photoinduced processes and the characteristics of the diffractive devices require some developmental work: firstly a theoretical model that could reproduce the diffraction intensities is needed; then, further studies are required to understand the permanent orientation of the liquid crystal domains.

The authors thank Prof. F. Simoni for helpful discussions. The work was supported by the Italian CIPE project 'Development of innovative materials for optics and electro-optics in civil and industrial applications', Cluster 26—P4, WP3 (innovative liquid crystals).

References

[1] Bunning, T. J., Natarajan, L. V., Tondiglia, V., Sutherland, R. L., Veziet, D. L., and Adams, W. W., 1995, *Polymer*, **36,** 2699.
[2] Natarajan, L. V., Sutherland, R. L., Tondiglia, V. P., Bunning, T. J., and Adams, W. W., 1996, *J. nonlin. Opt. Phys. and Mater*., **5,** 89.
[3] Fuh, A. Y.-G., Ko, T.-C., Tsai, M.-S., Huang, C. Y., and Chien, L.-C., 1998, *J. appl. Phys*., **83,** 679.
[4] Fuh, A. Y.-G., Tsai, M.-S., Huang, L. J., and Liu, T. C., 1999, *Appl. Phys. Lett*., **74,** 2572.
[5] Duca, D., Sukhov, A. V., and Umeton, C., 1999, *Liq. Cryst*., **26,** 931.
[6] Cipparrone, G., Mazzulla, A., and Simoni, F., 1998, *Opt. Lett*., **23,** 1505 and references therein.
[7] Simoni, F., Cipparrone, G., Mazzulla, A., and Pagliusi, P., 1999, *Chem. Phys*., **245,** 429.
[8] Cipparrone, G., Mazzulla, A., and Russo, G., 2001, *Appl. Phys. Lett*., **78,** 1186.
[9] Cipparrone, G., Mazzulla, A., and Russo, G., 2001, *J. opt. Soc. Am. B*, **18,** 1821.
[10] Di Bella, S., Lucchetti, L., and Simoni, F., 1999, *Mol. Cryst. liq. Cryst*., **373,** 191.
[11] Lucchetta, D. E., Francescangeli, O., Lucchetti, L., and Simoni, F., 2002, *Mol. Cryst. liq. Cryst*., **373,** 191.
[12] Nikolova, L., and Todorov, T., 1984, *Opt. Acta*, **31,** 579.
[13] Galabova, H. G., Allender, D. W., and Chen, J., 1997, *Phys. Rev. E*, **55,** 1627.
[14] Rajesh, K., Ram, M. K., Jain, S. C., Samanta, S. B., and Narliker, A. V., 1998, *Thin solid Films*, **325,** 251.